Nonreflecting Internal Wave Beam Propagation in the Deep Ocean

ROGER GRIMSHAW

Department of Mathematical Sciences, Loughborough University, Loughborough, United Kingdom

EFIM PELINOVSKY AND TATIANA TALIPOVA

Department of Nonlinear Geophysical Processes, Institute of Applied Physics, Nizhny Novgorod, Russia

(Manuscript received 7 November 2008, in final form 24 October 2009)

ABSTRACT

Using linear internal wave theory for an ocean stratified by both density and current, several background profiles are identified for which internal wave beams can propagate without any internal reflection. These special profiles are favorably compared with available oceanic data.

1. Introduction

It is well known that the stable background density stratification of the ocean interior allows for the vertical propagation of internal waves (e.g., Gill 1982). Furthermore, this process has been studied experimentally in the laboratory (e.g., Stevens and Imberger 1994). Moreover, it is also well known that a monochromatic internal wave is an exact solution of the fully nonlinear Euler equations for an unbounded stratified fluid (in the Boussinesq approximation) with a constant buoyancy (Brunt–Väisälä) frequency and such a wave propagates without change in amplitude and direction (e.g., Miropolsky 2001). In the general case when the buoyancy frequency varies with depth, an internal wave will transform and generate internal reflections. However, several observations (De Witt et al. 1986; Pingree and New 1989, 1991) and numerical simulations (Morozov and Pisarev 2002; Gerkema 2002, 2006; Gerkema et al. 2004; Johnston and Merrifield 2003; Holloway and Merrifield 2003; Vlasenko et al. 2003; Tabaei et al. 2005) of a nonlinear internal wave field in the ocean show that internal waves of tidal period propagate as beams with very weak internal reflection; indeed, no reflection is visible. Figure 1 demonstrates such behavior of internal wave beams (reflecting only between the sea surface and the bottom) in the Bay of Biscay (Gerkema et al. 2004). The existence of certain special buoyancy frequency profiles, in addition to the well-known case of a constant frequency, which allows for one-way propagation, has been previously noted in the literature [see, e.g., Magaard 1962; Krauss 1966; Vlasenko 1987; the recent book by Vlasenko et al. (2005)]. In this paper, we revisit this issue and analyze theoretically the penetration of internal waves in the ocean interior when there is a continuous stratification in background density and shear current. As well as recovering those already-known vertical profiles of the deep ocean stratification for which internal waves can propagate without any internal reflection, we find all such profiles, including some new ones. Further, we will show that these profiles can represent certain observed oceanic data rather well. Our theoretical results confirm that the internal reflection of internal waves in the deep ocean is generally quite weak when compared with the reflection from the ocean bottom and a near-surface pycnocline.

In section 2 we consider the case when the background stratification is solely due to the density field. Then in section 3 we extend this to the case when there is also a background shear current, although, for technical reasons, we consider only the nonrotating situation. In section 4, we examine the effect of wave reflection from a model of a near-surface pycnocline, which separates two different buoyancy frequency profiles. We conclude in section 5.

Corresponding author address: Roger Grimshaw, Department of Mathematical Sciences, Loughborough University, Loughborough LE11 3TU, United Kingdom.
E-mail: r.h.j.grimshaw@lboro.ac.uk

DOI: 10.1175/2009JPO4180.1

2. Internal waves in a density stratified ocean

The two-dimensional Euler equations for a density-stratified fluid in the Boussinesq approximation, when

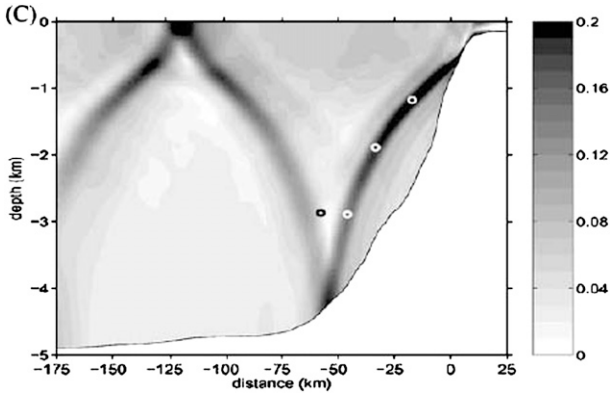

FIG. 1. Internal wave beams in the Bay of Biscay (Gerkema et al. 2004).

considered for a linear monochromatic wave of frequency ω, can be reduced to the wave equation (see, e.g., Le Blond and Mysak 1978):

$$\frac{\partial^2 W}{\partial x^2} - \alpha^2(z)\frac{\partial^2 W}{\partial z^2} = 0 \tag{1}$$

in which

$$\alpha^2(z) = \frac{\omega^2 - f^2}{N^2(z) - \omega^2}.$$

Here $W(x, z)$ is the vertical velocity of a water particle, $N(z)$ is the buoyancy frequency, f is the Coriolis parameter, z is the vertical coordinate (positive is downward), and x is the horizontal coordinate. Since (1) is a hyperbolic equation, we can introduce the characteristics (rays) for wave propagation:

$$\frac{dz}{dx} = \pm\alpha(z) = \pm\sqrt{\frac{\omega^2 - f^2}{N^2(z) - \omega^2}}, \tag{2}$$

where $\alpha(z) > 0$ and calculate the ray trajectories

$$x - x_0 = \int_{z_0}^{z} \frac{dz}{\alpha(z)}, \tag{3}$$

where x_0 and z_0 are the initial coordinates of the ray.

The propagation of internal wave beams has been extensively discussed in the literature, as cited in the introduction. These rays (or beams) are very visible in all computations of the internal wave field (including nonlinear computations). Indeed, these cited papers demonstrate the beam character of internal waves in the deep ocean, with a strong reflection from the sea surface and the sea bottom. However, it is well known that in general waves should exhibit internal reflection in an inhomogeneous medium (see, e.g., Brekhovskikh 1980; Rabinovich and Trubetskov 1989; Ostrovsky and Potapov 1999), and this seems to be rather weak for typical deep ocean conditions. This problem is considered in detail in the following analysis.

First, the existence of nonreflecting waves in the case of a constant buoyancy frequency is well known. The same situation is expected to hold approximately for the case of a slowly varying buoyancy frequency, presented as $N(\varepsilon z)$ with a small parameter ε representing the ratio of the wavelength to a characteristic vertical scale of variation of the buoyancy frequency. In this case, according to the WKB method (see, e.g., Bender and Orszag 1978; Brekhovskikh 1980; Rabinovich and Trubetskov 1989; Ostrovsky and Potapov 1999 for the general case; Baines 1995; Miropolsky 2001 for the internal wave context), the solution of (1) can be presented as

$$W(z, x) = A(\varepsilon z)\,\mathrm{Re}\{\exp[i(k_x x - \Psi(z))]\};$$
$$k_z(\varepsilon z) = \frac{d\Psi}{dz} \tag{4}$$

with two unknown real-valued functions: $A(\varepsilon z)$ and $k_z(\varepsilon z)$ for each fixed horizontal wavenumber k_x (>0). The equations for them are obtained by substituting (4) in (1) and separating the real and imaginary parts:

$$[k_x^2 - \alpha^2 k_z^2]A = -\varepsilon^2\alpha^2 A'', \tag{5}$$

$$2k_z A' + k_z' A = 0, \tag{6}$$

where a prime means a derivative with respect to the argument. Neglecting the term $O(\varepsilon^2)$ on the rhs of (5) but retaining (6) in full, the solution of these equations is found explicitly:

$$k_z(\varepsilon z) = \pm\frac{k_x}{\alpha(\varepsilon z)}; \quad k_z(\varepsilon z)A^2(\varepsilon z) = \text{const}. \tag{7}$$

The two signs in (7) correspond to a wave propagating in the downward or upward direction, respectively, where we have assumed that the z axis is vertically down. For definiteness, we consider an internal wave propagating downward so that its amplitude and vertical wavelength increase (decrease) as $N(z)$ decreases (increases) with depth. This asymptotic solution is valid for a slowly varying buoyancy frequency, and its derivation is well known. The expressions (7) are the leading-order terms in an asymptotic expansion, and in principle the expansion can be continued to an arbitrarily high order, with error $O(\varepsilon^{2n})$, while for an analytically smooth profile $N(\varepsilon z)$ the (internally) reflected wave is exponentially small $o[\exp(-C/\varepsilon^2)]$, where the constant C is found from the singularities of $N(\varepsilon z)$ in the complex plane (see, e.g.,

Bender and Orszag 1978; Boyd 1998). Although the reflected wave is vanishing small as ε goes to zero, it can have a significant amplitude in practice for finite nonzero values of ε.

Our goal here is to determine a large class of buoyancy frequency profiles for which an internal wave can propagate in the deep ocean with no internal reflection. That is, in essence, we seek to find those profiles for which the WKB solution can be made into an exact solution. Hereafter, the ordering parameter ε is omitted, as we are concerned with situations when it may not be small. It is convenient to use the construction of the WKB solution as a change of variables in (1):

$$W(z, x) = \alpha^{1/2}(z)V(Z, x); \quad Z = \int \frac{dz}{\alpha(z)}. \tag{8}$$

After substitution of (8), Eq. (1) transforms to

$$\frac{\partial^2 V}{\partial Z^2} - \frac{\partial^2 V}{\partial x^2} = Q(Z)V;$$

$$Q = -\alpha^{3/2}\frac{d^2\alpha^{1/2}}{dz^2} = \alpha^{1/2}\frac{d^2}{dZ^2}(\alpha^{-1/2}). \tag{9}$$

This equation coincides with Eq. (1.53) in the monograph by Vlasenko et al. (2005). In general, Eq. (9) is a variable-coefficient Klein–Gordon equation. The existence of waves without any internal reflection can now be achieved in the framework of a constant coefficient Eq. (9), which is possible if Q = const. In this case, the general solution of (9) is a superposition of Fourier components, $A(k_x, K)\exp(ik_x x + iKZ)$, where the dispersion relation, $k_x^2 = K^2 + Q$, has two distinct branches corresponding to upward and downward propagation, respectively. Further implications are discussed below. Other choices for $Q(Z)$ are possible, which also provide explicit closed-form expressions for V; however, in general, they will lead to internal reflections. For instance, the choice $Q \sim Z$ leads to a solution in terms of Airy functions, but these contain internally reflected waves with nonzero amplitudes (Bender and Orszag 1978).

There are three different cases when $Q(Z)$ can be constant, and each case describes a buoyancy frequency profile allowing an internal wave beam without internal reflection. We will discuss here only the buoyancy frequency profiles that decrease for large depths (i.e., the function $\alpha(z)$ tends to zero as z tends to infinity).

The first case is $Q = 0$, which leads to

$$\alpha(z) = p(1 + z/L)^2 \tag{10}$$

or

$$N(z) = \sqrt{\omega^2 + \frac{\omega^2 - f^2}{p^2(1 + z/L)^4}}, \tag{11}$$

where p and L are arbitrary constants; we note that L can be positive or negative in general. Mostly we will analyze the case $z > 0$ (in the deep ocean interior) and assume $L > 0$, but formally the obtained solution is also valid for negative z in the range $(-L < z < 0)$. The same solution can be used for a subsurface layer (above the pycnocline) considering $z < 0$ and $L < 0$.

The general solution of (9) for $Q = 0$ consists of two independent waves propagating in opposite directions:

$$V(Z, x) = F_1(x - Z) + F_2(x + Z). \tag{12}$$

Formally, the buoyancy frequency profile (11) was obtained already in the literature (Vlasenko 1987; Vlasenko et al. 2005), but its explicit interpretation as a ''nonreflecting'' beam was not made. Here we will use this nonreflecting wave beam to describe the deep penetration of internal waves in the ocean. Moreover, owing to (8), the wave amplitude increases at large depths where the buoyancy frequency decreases.

The rays in the ocean with this nonreflecting buoyancy frequency (11) can be calculated explicitly:

$$p(x - x_0) = \frac{z}{1 + z/L}, \tag{13}$$

and they have a vertical asymptote for large depths. In the limiting case of low-frequency internal waves in a nonrotating ocean, the nonreflecting profile is the same for waves of different frequencies:

$$N_e(z) = \frac{N_0}{(1 + z/L)^2}. \tag{14}$$

Here $N_0 = N_e(0)$ is arbitrary constant, and the wave parameters vary as

$$A_e(z) = A_0(1 + z/L); \quad k_z(z) = \frac{N(z)}{c} = \frac{N_0}{c(1 + z/L)^2}, \tag{15}$$

where $c = \omega/k_x$ is the wave speed in the horizontal direction and A_0 is initial wave amplitude.

The second class of profiles can be obtained from the condition $Q = m^2 > 0$. In this case, the equation for α in (9) is integrated once,

$$\left(\frac{d\sqrt{\alpha}}{dz}\right)^2 - \frac{m^2}{\alpha} = E, \tag{16}$$

where E is a constant, and then the solution for α can be found by quadature. In particular, if $E = 0$, its solution is

$$\alpha(z) = 2mz + C_1, \tag{17}$$

where C_1 is an arbitrary constant. This rather simple solution appears to be new. If $E \neq 0$, the general solution is

$$\alpha(z) = \frac{(Ez + C_2)^2 - m^2}{E}. \tag{18}$$

This solution generalizes (10) for $m = 0$, and it was found by Vlasenko (1987); see also the recent monograph by Vlasenko et al. (2005).

Alternatively, the special solution (17) for $\alpha(z)$ can be easily directly obtained from (9) and is

$$\alpha(Z) = \alpha_0 \exp(2mZ); \quad z(Z) = \int \alpha(Z)\, dZ$$

so that

$$\alpha(z) = p(1 + z/L), \tag{19}$$

where $p = C_1 = 2mL$. Then

$$N(z) = \sqrt{\omega^2 + \frac{\omega^2 - f^2}{p^2(1 + z/L)^2}}. \tag{20}$$

The rays in this model of a nonreflecting buoyancy frequency are described by

$$p(x - x_0) = L \ln(1 + z/L). \tag{21}$$

Now the rays have no vertical asymptote for large depths but slowly turn to the vertical. In the limiting case of low frequency waves in a nonrotating ocean, the nonreflecting profile of the buoyancy frequency is

$$N_e(z) = \frac{N_0}{1 + z/L}. \tag{22}$$

It differs from (14) in that it provides a slower change of the buoyancy frequency with depth.

The elementary downward-traveling wave solution of the Klein–Gordon Eq. (9) with a positive Q has a sinusoidal shape,

$$V(x, Z) = V_0 \sin[k_x x - K_z Z]; \quad K_z = \sqrt{k_x^2 - m^2} \tag{23}$$

if $k_x > m$. In the opposite case, the wave exponentially attenuates with depth. The general solution for a traveling wave is obtained by Fourier superposition of the elementary solutions (23),

$$V(x, Z) = \int V_0(k_x) \exp\{i[k_x x - K_z(k_x)Z]\}\, dk_x, \tag{24}$$

where K_z and k_x satisfy the dispersion relation (23). As a result, the wave field is now dispersive and the beamwidth increases with depth.

Next, the general solution (18) can also be obtained directly from (9) as follows:

$$\alpha(Z) = \alpha_0 \operatorname{sech}^2(mZ)$$

or

$$\alpha(Z) = \alpha_0 \operatorname{cosech}^2(mZ) \tag{25}$$

so that

$$\alpha(z) = p[1 - q^2(1 + z/L)^2] \quad \text{or}$$
$$\alpha(z) = p(q^2(1 + z/L)^2 - 1), \tag{26}$$

where $pq = mL$. These equations agree with (18) after putting $pq^2 = \mp EL^2$, respectively. We see that the first solution has $E < 0$, and, since we require that $\alpha > 0$, it is only valid for a finite range of z, and consequently not very useful. The second solution has $E > 0$ and $\alpha > 0$ for all z if $q > 1$; but comparison with the observations discussed below show that there is not a significant difference from the profile (11), which has the same asymptotic behavior for large $|z|$. Hence, we will not consider either of these profiles any further here.

The third class of profiles can be obtained from the condition $Q = -m^2 < 0$. In this case, the solution for $\alpha(z)$ is also found explicitly ($E > 0$):

$$\alpha(z) = \frac{(Ez + C_2)^2 + m^2}{E} \tag{27}$$

or

$$\alpha(Z) = \alpha_0 \sec^2(mZ + \varphi)^2; \quad \alpha(z) = p(1 + z^2/L^2), \tag{28}$$

where $pq = mL$ and $pq^2 = EL^2$. The nonreflecting buoyancy frequency profile in this case is described by

$$N(z) = \sqrt{\omega^2 + \frac{\omega^2 - f^2}{p^2[1 + z^2/L^2]^2}}. \tag{29}$$

For $z > 0$ the solution (29) is a monotonically decreasing function of depth. Equation (29) was obtained by Vlasenko 1987 (see also Vlasenko et al. 2005) in the context of finding the modal structure of the internal tide. At large depths the asymptotic $\alpha(z) \sim z^{-2}$ is valid, as in the case (11). It is important to mention that this

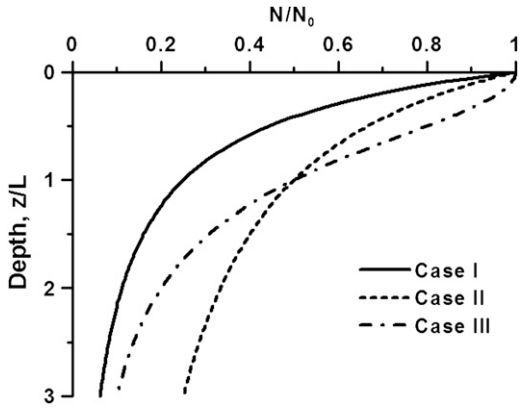

FIG. 2. Nonreflected profiles of the buoyancy frequency.

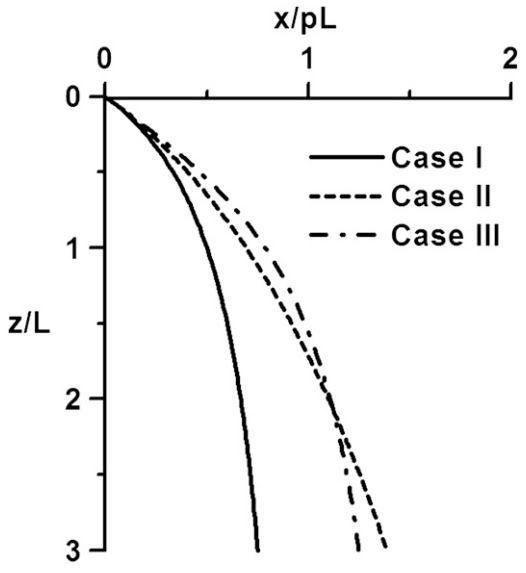

FIG. 3. Rays for various nonreflected profiles of the buoyancy frequency.

obtained solution can describe the buoyancy frequency profile in the vicinity of a pycnocline (if its center is located at $z = 0$), and this is the first example of a nonmonotonic nonreflecting profile. The wave field again has the shape (24), but the dispersion relation is now

$$K_z = \sqrt{k_x^2 + m^2} \tag{30}$$

with no formal limitations on the value of k_x. In this case the beamwidth again increases with depth. The rays in this model of a nonreflecting buoyancy frequency are

$$p(x - x_0) = \frac{q}{L} \tan^{-1}[q(1 + z/L)], \tag{31}$$

and the rays again have a vertical asymptote for large depths. In the limiting case of low frequency waves in a nonrotating ocean, the nonreflecting profile of the buoyancy frequency in this third case is

$$N_e(z) = \frac{N_0}{1 + z^2/L^2}, \tag{32}$$

which has the same asymptotic behavior as (14).

Thus, we have found four cases of a nonreflecting internal wave beam propagation in the deep ocean. The classical example $N = \text{const}$ can be obtained from (14) as $L \to \infty$ (as formally from all other profiles): here it will be not analyzed separately. In the case of (14) (which will be called case I below), the wave shape does not vary with depth (but the wave amplitude and wavelength do change with depth) and the beamwidth remains constant. In the cases (22) and (32) (called case II and case III, respectively), the beamwidth again increases with depth.

All nontrivial nonreflecting profiles in the low frequency limit (in variables N/N_0 and z/L) are presented in Fig. 2. In case I, the profile (14) corresponds to a faster decrease of the buoyancy frequency with depth; in case II, the profile (22) varies slowly with depth; and in case III, the profile (32) tends to (14) for large depths but is only slowly varying for small depths. The rays for the same nonreflecting buoyancy frequency profiles are displayed in Fig. 3. All curves are qualitatively the same, but their asymptotic behaviors for large depths are different.

A comparison of observed profiles of the buoyancy frequency with the nonreflecting profiles (14), (22), and (32) is given in Fig. 4 for the Pacific, Atlantic, Indian, and Arctic Oceans. Figure 4a shows results of measurements on the North West Shelf (NWS) of Australia in the Indian Ocean at 20°S (Holloway et al. 1997; Holloway 2001); the Malin shelf edge stratification in the Northern Atlantic (56.5°N) is illustrated in Fig. 4b (Pelinovsky et al. 1999; Grimshaw et al. 2004); the third example (Fig. 4c) is the buoyancy profile on the Hawaiian Ridge in the Pacific Ocean at 22°N (Johnston and Merrifield 2003); the last example (Fig. 4d) is for the Laptev Sea in the Arctic Ocean at 73°N (Polukhin et al. 2003a,b; Grimshaw et al. 2004). In all figures the vertical coordinate z is measured from the center of the pycnocline. The theoretical nonreflecting profiles of the buoyancy frequency (14), (22), and (32), computed for the semidiurnal (M_2) tide (12.4 h), are also presented in Fig. 4. The fitting parameters are given in Table 1 for all three cases (for the Laptev Sea, L is given above/below the pycnocline).

From Fig. 4a for the NWS of Australia, the second fit (22) (green dashed–dotted line) seems to be the best, but the first fit (14) (red dashed line) may also be used for a description of this buoyancy frequency profile. Again, from Fig. 4b for the Malin shelf edge stratification, the best fit seems to be the second approximation (22) (green

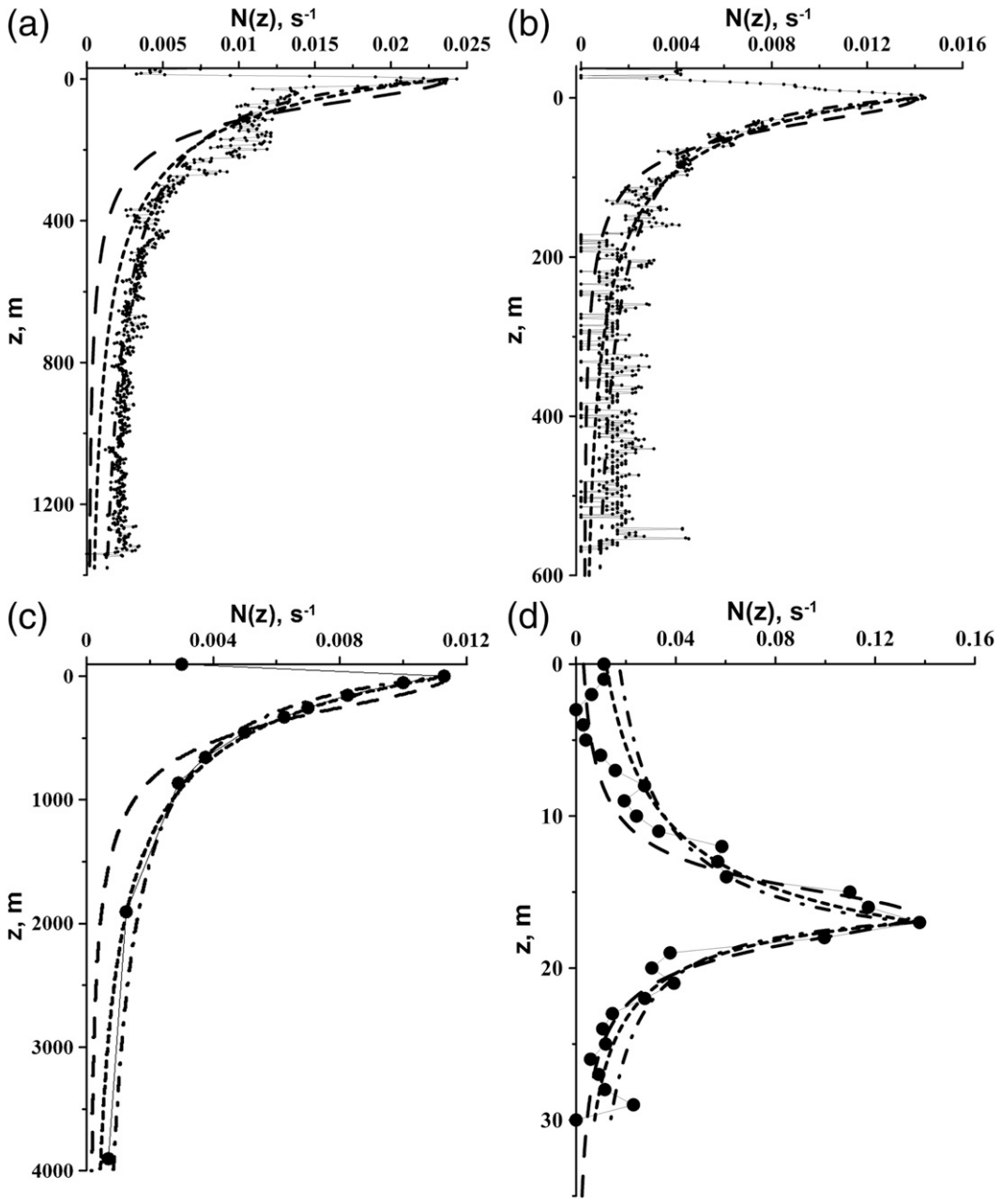

FIG. 4. Buoyancy frequency profile and its approximation by a nonreflecting profile: (a) North West Shelf of Australia, (b) Malin shelf edge, (c) Hawaiian Ridge, and (d) Laptev Sea. Dashed lines is fit (14), dashed–dotted lines is fit (22), and dotted lines is fit (32); lines with points are the measured data.

dashed–dotted line); however, both other approximations (14) (red dashed line) and (32) (purple dotted line) may be used. For the Hawaiian Ridge (Fig. 4c) we see that both fits, the first (14) (red dashed line) and the second (22) (green dashed–dotted line) describe the buoyancy frequency profile quite well, but the third fit (32) (purple dotted line) is not so good. The third fit (32) (purple dotted line) describes the buoyancy frequency profile in the Laptev Sea (both above and below the pycnocline). Also, the density stratification for the Laptev Sea is fitted by the profiles of cases I and II with different values of L above and below the pycnocline; see Table 1 where in the Laptev Sea case the slash denotes the values of L above/below the pycnocline. So, all theoretical nonreflected profiles can be used to fit the measured data.

It is important to mention that all of the theoretical profiles—(11), (20), and (29)—formally include a dependence on the wave frequency; therefore, for a fixed

TABLE 1. Fitting parameters of nonreflecting buoyancy frequency profiles.

			Case I		Case II		Case III	
	N_0 (s^{-1})	Depth (m)	L (m)	$1/p$	L (m)	$1/p$	L (m)	$1/p$
NWS of Australia	0.024	1380	230	180	82	180	100	180
Malin shelf edge	0.0144	606	105	195	35	195	45	195
Hawaii Ridge	0.0113	4000	950	88	320	88	390	88
Laptev Sea	0.1378	30	7.15/4	7000	2.5/1.5	7000	2.5	7000

stratification, only one wave with the appropriate frequency will be have no internal reflections. However, this dependence is negligible for the Malin shelf edge (Fig. 5) where the buoyancy frequency profile is fitted by formula (20) for three different wave periods T: semidiurnal tide ($T = 12.4$ h), $T = 6.2$ h, and $T = 4.1$ h. All profiles almost coincide; therefore, various spectral components of the low-frequency internal wave field propagate at depth with no internal reflection.

Thus, our theoretical analysis shows the existence of several density stratifications in the ocean that can provide nonreflecting propagation of internal waves in the deep ocean. Further, we have shown that the observed density stratification in various areas of the world's oceans can be fitted by these profiles. This means that the vertical propagation of internal waves with minimal internal reflection is typical for real oceans, thus explaining the results of various numerical simulations cited in the introduction.

3. Traveling waves in an ocean stratified in density and current

The same approach can be applied for the propagation of internal waves in an ocean with both density and current stratification. For simplicity we consider here monochromatic low-frequency waves in a nonrotating ocean for which the basic equation for the vertical velocity (or streamfunction) reduces to the Taylor–Goldstein equation (see, e.g., Baines 1995; Miropolsky 2001),

$$\frac{d^2w}{dz^2} + \kappa^2(z)w = 0, \tag{33}$$

where

$$\kappa^2(z) = \frac{N^2(z)}{(c - U(z))^2} + \frac{1}{c - U(z)}\frac{d^2U}{dz^2}. \tag{34}$$

Here $U(z)$ is the background shear flow (assumed stable) and c is the wave speed in the horizontal direction. Using again the WKB construction,

$$V = \kappa^{1/2}(z)w; \quad Z = \int \kappa(z)\, dz, \tag{35}$$

Eq. (33) reduces to

$$\frac{d^2V}{dZ^2} + V = Q(Z)V; \quad Q(Z) = \frac{1}{\kappa^{1/2}(Z)}\frac{d^2}{dZ^2}[\kappa^{1/2}(Z)]. \tag{36}$$

Nonreflecting wave solutions are obtained from (36) if Q does not depend on Z and

$$-\infty < Q < 1. \tag{37}$$

Again three classes of background profiles are possible.

The first case is $Q = 0$, leading to

$$\frac{N^2(z)}{[c - U(z)]^2} + \frac{1}{c - U(z)}\frac{d^2U}{dz^2} = \frac{\kappa_0^2}{(1 + z/L)^4}, \tag{38}$$

which determines a relationship between $N(z)$ and $U(z)$. So, the main difference with the previous cases is that

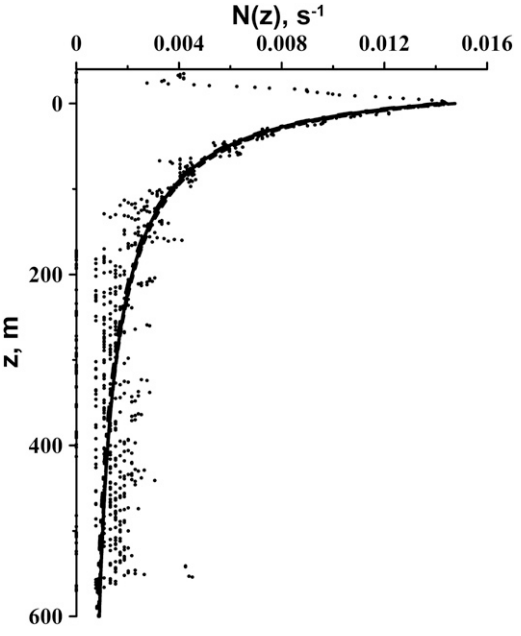

FIG. 5. Buoyancy frequency profile and its approximation by the nonreflecting profile (20) for the Malin shelf edge: $T = 12.4$ h (solid line), $T = 6.2$ h (dashed line), and $T = 4.1$ h (dashed line with dots); the black line is the experimental data.

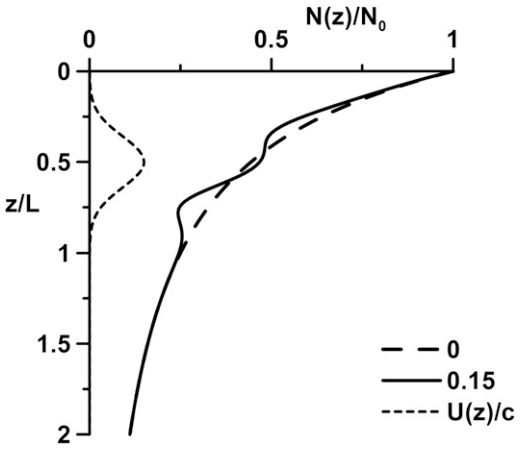

FIG. 6. Nonreflecting buoyancy profile in a basin with a shear flow: numbers are values of U/c.

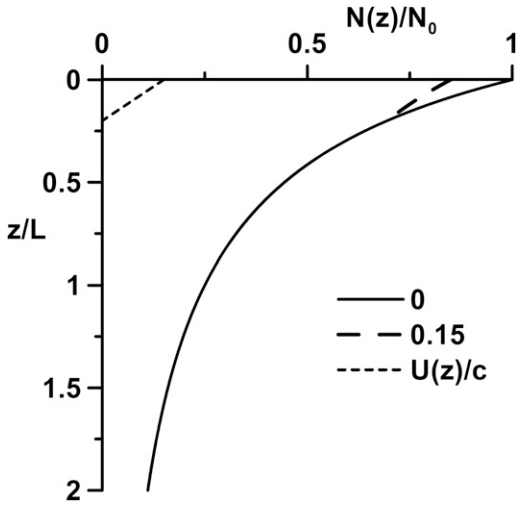

FIG. 7. Nonreflecting buoyancy profile in a flow with a constant shear: numbers are values of U/c.

now there is an infinite number of background density and shear flow stratifications providing nonreflecting propagation of internal waves in the deep ocean. For each density profile $N(z)$ from (38) we can find the corresponding shear flow $U(z)$, in principle. However, Eq. (38) with respect to $U(z)$ is a second-order linear ordinary differential equation with variable coefficients, and to find its analytical solutions is very difficult. It is simpler is to find $N(z)$ from (38) for a given $U(z)$.

If the shear flow has the Gaussian shape, shown in Fig. 6,

$$U(z) = u \exp\left[-\frac{(z - z_0)^2}{l^2}\right]: \tag{39}$$

the computed buoyancy profile satisfied to (34) is displayed in Fig. 6 for $l/L = 0.2$, $z_0/L = 0.5$, $c^2/l^2N_0^2 = 0.3$. It is clearly seen that the nonreflecting buoyancy profile is deformed in the zone of the shear flow with some fine structure. Such structure is visible on many observed profiles (see Fig. 4) and they, together with the shear flow (which is very often not measured together with the density profile), can provide nonreflecting downward propagation of an internal wave in the ocean interior.

Another example is the flow with a constant shear in the subsurface layer:

$$U(z) = \begin{cases} u(1 - z/l), & 0 < z < l \\ 0, & l < z < L \end{cases}. \tag{40}$$

The nonreflecting buoyancy profile is modified in the subsurface layer also (Fig. 7 for $l/L = 0.2$ and $u/c = 0.15$). In fact, the point $z = l$ is singular (U_{zz} is infinite), and the stratification should be smoothed in the vicinity of this point.

If the background is weak, all nonreflecting density profiles are described approximately by

$$\frac{N(z) - N_0(z)}{N_0(z)} \approx -\frac{U(z)}{c} - \frac{c}{2N_0^2(z)}\frac{d^2U}{dz^2}, \tag{41}$$

obtained from (38) at the first order of a perturbation theory. Here $N_0(z)$ is the nonreflecting profile (14) with no background shear flow. In zones of weak density stratificationeven a smooth shear flow leads to strong variability of the buoyancy frequency profile.

Especially we would like to note the solution of (38) for $L \to \infty$ (that is κ is a constant). If there is no shear flow, this case corresponds to the classical case of constant buoyancy frequency, providing propagation of a wave with constant amplitude. If the shear is constant (dU/dz = const), the same result holds when $N(z)/(c - U(z))$ is a constant; namely, an internal wave propagates with no reflection.

The second case is $0 < Q < 1$ when $\kappa(z)$ is described by an expression analogous to (38) and the relation between $N(z)$ and $U(z)$ is

$$\frac{N^2(z)}{(c - U(z))^2} + \frac{1}{c - U(z)}\frac{d^2U}{dz^2} = \frac{\kappa_0^2}{(1 + z/L)^2}. \tag{42}$$

Formally, $\kappa_0 L > ½$ is needed to ensure that $Q < 1$. This limitation occurred also for the case with density stratification only; see (17). It is important to note that in the case of a weak current, the expression (41) is again valid; however, now $N_0(z)$ satisfies (22).

In the third case ($Q < 0$), Eq. (42) is replaced on

$$\frac{N^2(z)}{[c - U(z)]^2} + \frac{1}{c - U(z)}\frac{d^2U}{dz^2} = \frac{\kappa_0^2}{1 + (z/L)^2}. \tag{43}$$

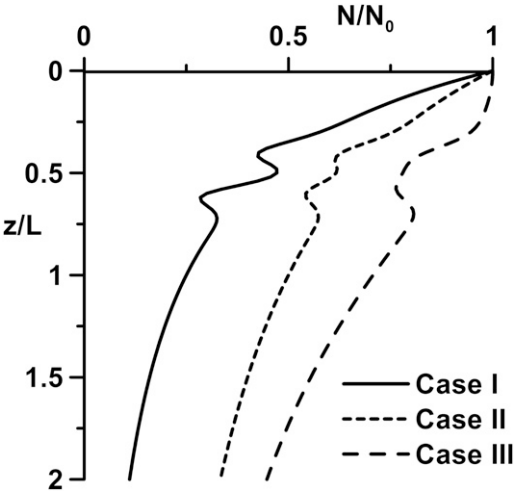

FIG. 8. Nonreflecting buoyancy profiles with a Gaussian-shaped current.

Again, for a weak current the expression (41) is valid, with $N_0(z)$ now satisfying (32).

Figure 8 demonstrates the influence of a current with the Gaussian shape (39) on the nonreflecting buoyancy profile for all three cases described by (38), (42), and (43) for $l/L = 0.1$, $z_0/L = 0.5$, $c^2/l^2N_0^2 = 0.3$, $u/c = 0.2$. It can be seen that the perturbations of the buoyancy profile are different, and such perturbations are sensitive to the shape of the unperturbed buoyancy profile.

There is also an alternative approach to that described above in which we assume at the outset that the current shear is weak, so we replace (34) with

$$\kappa(z) = \frac{N(z)}{c - U(z)}. \tag{44}$$

Then the same change of variables (35) leads to

$$\frac{d^2V}{dZ^2} + V = Q(Z)V,$$

where now

$$Q(Z) = \frac{1}{\kappa^{1/2}(Z)}\frac{d^2}{dZ^2}[\kappa^{1/2}(Z)] - \frac{(\kappa U_Z)_Z}{\kappa(c-U)}. \tag{45}$$

Essentially the former procedure placed the term involving the curvature U_{zz} into the phase of the wave, whereas now we place it in the amplitude of the wave. The simple choice $Q = 0$ leads to the solution

$$B = \kappa^{1/2}(c - U),$$

where

TABLE 2. The coefficient of internal wave reflection on the pycnocline.

	N_0 (s^{-1})	H (m)	L_p (m)	C (m s^{-1})	$\lvert R\rvert^2$
NWS of Australia	0.0236	1380	18.5	2.1	0.81
Malin shelf edge	0.0144	606	28	0.43	0.22
Hawaiian Ridge	0.0113	4000	111.1	2.0	0.53
Laptev Sea	0.1378	30	2.5	0.75	0.55

$$\frac{d^2B}{dz^2} = 0. \tag{46}$$

The choice $B = \text{const}$ leads to $N(c - U) = \text{const}$, which generalizes the classical case when $N(z) = \text{const}$. Otherwise, the choice $B = B_0Z$ leads to the solution

$$\kappa(c-U)^2 = N(c-U) = \frac{B_0^2}{\xi^2}; \quad \xi = -\frac{1}{Z} = \int_{z_0}^{z} \frac{dz}{(c-U)^2}. \tag{47}$$

This generalizes the case when $Q = 0$ leads to (10) in section 2. Overall, this alternative class of nonreflecting buoyancy profiles will exhibit qualitatively the same sensitivity to the presence of even a rather small shear flow, as for the cases we have discussed above.

4. Reflection properties of a pycnocline

If the background stratification differs from any of the nonreflecting profiles given above, the internal wave will reflect in the ocean interior. This effect is important for the passage of an internal wave through a pycnocline where there is typically a fast variation of the buoyancy frequency. We consider here a simplified example of internal wave reflection from a pycnocline in the ocean interior, for the nonrotating case, where the pycnocline is modeled as a superposition of two nonreflecting profiles (14),

$$N(z) = N_0 \begin{cases} \dfrac{1}{(1 + |z|/L_1)^2}, & z < 0 \\ \dfrac{1}{(1 + z/L_2)^2}, & z > 0 \end{cases} \tag{48}$$

with different characteristic scales. As shown in Fig. 4, this distribution of the buoyancy frequency may be used for the approximation of many observed profiles. The fitted parameters are given in Table 2 and are used here for the quantitative estimation of wave reflection from the pycnocline. For simplicity, we will ignore in this section any effects of a shear flow and use the low frequency approximation.

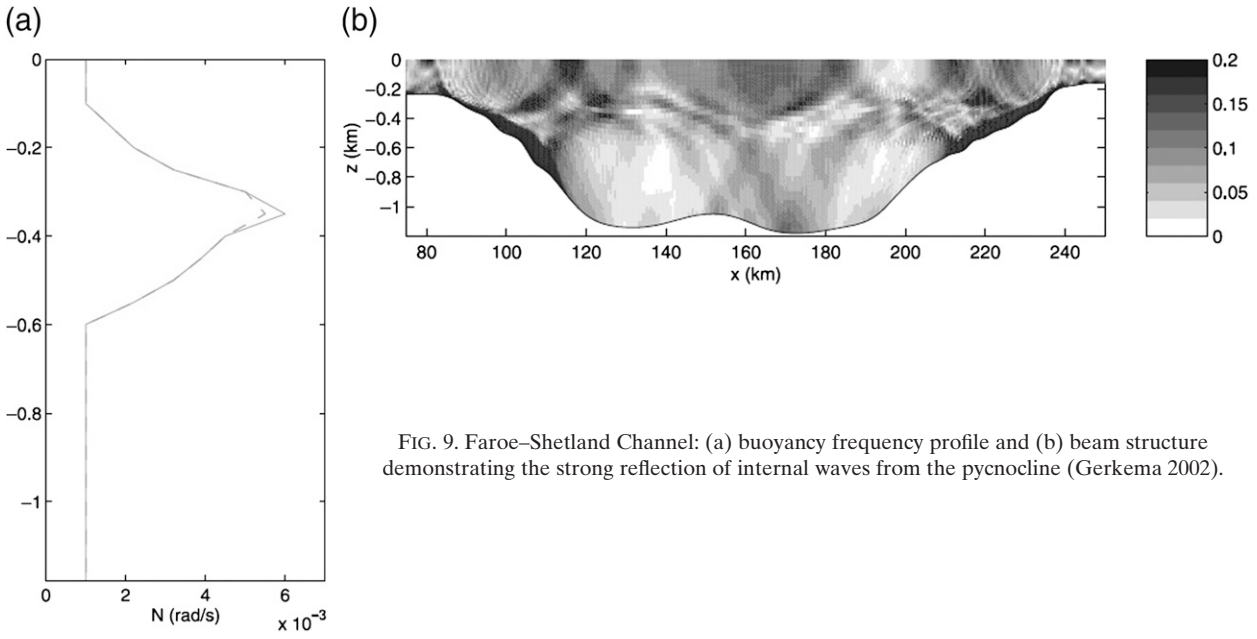

FIG. 9. Faroe–Shetland Channel: (a) buoyancy frequency profile and (b) beam structure demonstrating the strong reflection of internal waves from the pycnocline (Gerkema 2002).

Let an internal wave be incident on the pycnocline from $z < 0$. Writing the solution of the wave equation (1) as the sum of incident and reflected waves above the pycnocline and a transmitted wave below it and using continuity conditions for the vertical velocity and its derivative at the point $z = 0$, we find the reflection coefficient in the form

$$R = -\frac{1}{1 + 2iN_0L_p/c}, \tag{49}$$

where $L_p = L_1L_2/(L_1 + L_2)$. The complex value of R is the ratio of the amplitude of reflected wave to the amplitude of the incident wave at $z = 0$ (away from this point, the amplitudes grow linearly with distance). The modulus of R is

$$|R| = \frac{1}{(1 + 4N_0^2L_p^2/c^2)^{1/2}}. \tag{50}$$

When the pycnocline depth is much less than the ocean depth, the modulus of the reflection coefficient tends to 1 (strong reflection). In a ''shallow'' ocean when the pycnocline depth is comparable with the ocean depth, the modulus of the reflection coefficient may be quite weak. In general, $|R|^2$ characterizes the energy of the reflected wave. This coefficient is computed for all of the buoyancy frequency profiles presented in Fig. 4. The speed c in each case is found as the maximum value of the wave speed in the horizontal direction computed from the eigenvalue problem,

$$\frac{d^2w}{dz^2} + \frac{N^2(z)}{c^2}w = 0, \tag{51}$$

with zero values on the sea surface and sea bottom. The results of these calculations are presented in Table 2. The value of $|R|^2$ is quite large for the North West Shelf off Australia and is about 0.5 for the Hawaiian Ridge and the Laptev Sea. It equals 0.22 for the Malin shelf edge. So, overall, internal waves are reflected from the pycnocline (and, of course, from sea surface and sea bottom). An example of strong reflection from a pycnocline computed for the Faroe–Shetland Channel is shown in Fig. 9 (taken from Gerkema 2002).

In fact, the reflection properties of a pycnocline are sensitive to the shape of the pycnocline. For instance, if the pycnocline in the Laptev Sea is approximated by (32) (case III), there is no reflection. In this case, use of the buoyancy profile (14) (case I) can give an upper limit of the reflection coefficient due to the large value of the jump in dN/dz at the center of the pycnocline.

5. Conclusions

Observed data and numerical simulations typically demonstrate the deep penetration of internal wave beams in the interior of the ocean with no visible internal reflection (except rather strong reflections from the sea surface, pycnocline, and the sea bottom). Although this effect may be related to the rather slow spatial variation of the buoyancy frequency with depth

relative to the wavelength of the wave beam, in this paper we have argued that another possible explanation is related to the existence of several families of ''nonreflecting'' background profiles in density and current. We have described a full set of such profiles, found within the framework of the linearized theory for internal waves in a stratified fluid. In the absence of a background shear flow, three possible profiles of the buoyancy frequency are found. In case I the buoyancy frequency below the pycnocline is described by $(1 + z/L)^{-2}$ and the wave shape remains constant with depth, but its amplitude and wavelength vary with depth; the wave field is concentrated in beams. The well-known example of nonreflecting wave propagation in an ocean with a constant buoyancy frequency is a particular case for $L \to \infty$. In case II the buoyancy frequency profile is described by $(1 + z/L)^{-1}$, and the internal wave beam increases its width with depth. In case III the buoyancy frequency profile is nonmonotonic $[1 + (z/L)^{-2}]^{-1}$ and can describe the structure of an internal pycnocline. The beamwidth in this case is also increased.

Observed buoyancy frequency profiles in many areas of the world's oceans can, in many cases, be well approximated by the nonreflecting profiles obtained. We have demonstrated this here for the North West Shelf of Australia, the Malin shelf edge, the Hawaiian Ridge, and the Laptev Sea. This good fitting of observed data by the theoretical profiles allows us to conclude that nonreflecting beam propagation of the internal waves in the ocean is a frequent phenomenon and not necessarily dependent on the slow variation of the buoyancy frequency with depth.

If the ocean is stratified in both density and current, we have found that there is an infinite number of nonreflecting background profiles allowed. In fact, for each density profile one can find an associated nonreflecting shear flow: some examples of such profiles are given in this paper. In practice, the background density and current profiles are arbitrary, constrained only by the thermal wind relation. Although the nonreflecting density and current profiles are linked in the present theory, the fact that there is an infinite set of such profiles allows us to conclude that observed profiles can be well approximated by a nonreflecting profile.

At a pycnocline, where the buoyancy frequency varies significantly, a downward-propagating internal wave reflects. The reflection coefficient is calculated for the North West Shelf of Australia, Malin shelf edge, Hawaiian Ridge, and Laptev Sea. We find that it varies over a wide range and is sensitive to the details of stratification in the vicinity of the pycnocline. It is also demonstrated that, if the buoyancy profile in the vicinity of the pycnocline is symmetrical and described by the profile (28) (case III), the internal wave can pass through a pycnocline with no reflection.

The nonreflecting buoyancy frequency profiles have been obtained here in the framework of the linearized theory of internal waves. It is well known that in the case of $N(z) = \text{const}$, the nonlinear wave also propagates without reflection. The analysis of nonlinear downward propagation of internal waves will be given in a future study. But it is pertinent to note in this context that nonlinear theories for slowly varying internal gravity waves have demonstrated that the main nonlinear effect is the generation of a wave-induced mean flow (e.g., Grimshaw 1974, 1975; Sutherland. 2006). Since we have shown that the class of nonreflecting profiles can, in principle, allow for arbitrary background shear flow, we expect that the results obtained here may indeed extend to the nonlinear case. Further, as we have shown above, the results of observations and numerical simulations made for real parameters of the internal wave field demonstrate the beam character of the wave propagation, irrespective of the nonlinearity of the wave amplitude.

The solutions described above can also be used to compute the modal structure of an internal wave field in an ocean of finite depth H, as described in Vlasenko et al. (2005) for the case $Q = 0$ [see (11)]. In this case, the vertical structure of the internal wave satisfying zero boundary conditions at the sea surface ($z = 0$) and bottom ($z = H$) can be presented explicitly, when $Q = 0$, $\pm m^2$, for cases I, II, and III as

$$W_n(z) = B\alpha_n^{1/2}(z)\sin[\Psi_n(z)], \quad \Psi_n(Z) = (k_x^2 - Q)^{1/2}Z,$$

$$\Psi_n(H) = 2\pi n, \quad Z = \int_0^z \frac{dz}{\alpha_n(z)},$$

and

$$\alpha_n(z) = \sqrt{\frac{\omega_n^2 - f^2}{N^2(z) - \omega_n^2}}, \tag{52}$$

respectively, where $n = 1, 2, 3, \ldots$ is the modal number and B is a normalizing constant [see (8) and (9)]. This leads to the dispersion relation for an internal wave mode

$$\sqrt{k_x^2 - Q}\int_0^H \frac{dz}{\alpha_n(z)} = 2\pi n. \tag{53}$$

Acknowledgments. Grants from INTAS (06-1000013-9236) and RFBR (08-05-91850-KO_a) for all coauthors, Leverhulme Trust for EP, and RFBR (09-05-00204 and 07-05-392310-HBO_a) for TT are acknowledged.

REFERENCES

Baines, P. G., 1995: *Topographic Effects in Stratified Flows*. Cambridge University Press, 482 pp.

Bender, C. M., and S. A. Orszag, 1978: *Advanced Mathematical Methods for Scientists and Engineers*. McGraw-Hill, 593 pp.

Boyd, J. P., 1998: *Weakly Nonlocal Solitary Waves and Beyond-All-Orders Asymptotics*. Mathematics and its Applications, Vol. 442, Kluwer, 590 pp.

Brekhovskikh, L. M., 1980: *Waves in Layered Media*. Academic Press, 503 pp.

De Witt, L. M., M. D. Levine, C. A. Paralson, and W. W. Burt, 1986: Semidiurnal internal tide in JASIN: Observations and simulation. *J. Geophys. Res.,* **91,** 2581–2592.

Gerkema, T., 2002: Application of an internal tide generation model to baroclinic spring-neap cycles. *J. Geophys. Res.,* **107,** 3124, doi:10.1029/2001JC001177.

——, 2006: Internal-wave reflection from uniform slopes: Higher harmonics and Coriolis effects. *Nonlinear Processes Geophys.,* **13,** 265–273.

——, F. A. Lam, and L. R. M. Maas, 2004: Internal tides in the Bay of Biscay: Conversion rates and seasonal effects. *Deep-Sea Res. II,* **5,** 12 995–13 008.

Gill, A. E., 1982: *Atmosphere-Ocean Dynamics*. International Geophysics Series, Vol. 30, Academic Press, 662 pp.

Grimshaw, R., 1974: Internal gravity waves in a slowly varying dissipative medium. *Geophys. Fluid Dyn.,* **6,** 131–148.

——, 1975: Nonlinear internal gravity waves and their interaction with the mean wind. *J. Atmos. Sci.,* **32,** 1779–1793.

——, E. Pelinovsky, T. Talipova, and A. Kurkin, 2004: Simulation of the transformation of internal solitary waves on oceanic shelves. *J. Phys. Oceanogr.,* **34,** 2774–2791.

Holloway, P. E., 2001: A regional model of the semidiurnal internal tide on the Australian North West Shelf. *J. Geophys. Res.,* **106** (C6), 19 625–19 638.

——, and M. A. Merrifield, 2003: On the spring-neap variability and age of the internal tide at the Hawaiian Ridge. *J. Geophys. Res.,* **108,** 3126, doi:10.1029/2002JC001486.

——, E. Pelinovsky, T. Talipova, and B. Barnes, 1997: A nonlinear model of internal tide transformation on the Australian North West shelf. *J. Phys. Oceanogr.,* **27,** 871–896.

Johnston, T. M. S., and M. A. Merrifield, 2003: Internal tide scattering at seamounts, ridges, and islands. *J. Geophys. Res.,* **108,** 3180, doi:10.1029/2002JC001528.

Krauss, B., 1966: *Interne Wellen*. Gebrüder Borntraeger, 248 pp.

Le Blond, P. H., and L. A. Mysak, 1978: *Waves in the Ocean*. Elsevier, 602 pp.

Magaard, L., 1962: Zur berechnung interner wellwn in meeresräumen mit night-ebenen böden bei einer speziellen dichteverteilung. *Kiel. Meeresforsch.,* **18,** 161–183.

Miropolsky, Yu. Z., 2001: *Dynamics of the Internal Gravity Waves in the Ocean*. Kluwer, 406 pp.

Morozov, E. G., and S. V. Pisarev, 2002: Internal tides at the arctic latitudes (Numerical experiments). *Oceanology,* **42,** 153–161.

Ostrovsky, L. A., and A. I. Potapov, 1999: *Modulated Waves: Theory and Applications*. The John Hopkins University Press, 369 pp.

Pelinovsky, E., T. Talipova, and J. Small, 1999: Numerical modelling of the evolution of internal bores and generation of internal solitons at the Malin shelf. The 1998 WHOI/IOS/ONR internal solitary wave workshop: Contributed papers, T. F. Duda and D. M. Farmer, Eds., Tech. Rep. WHOI-99-07, 229–236.

Pingree, R. D., and A. L. New, 1989: Downward propagation of internal tidal energy into the Bay of Biscay. *Deep-Sea Res.,* **36A,** 735–758.

——, and ——, 1991: Abyssal penetration and bottom reflection of internal tide energy in the Bay of Biscay. *J. Phys. Oceanogr.,* **21,** 28–39.

Polukhin, N., T. Talipova, E. Pelinovsky, and I. Lavrenov, 2003a: Kinematic characteristics of the high-frequency internal wave field in the Arctic Ocean. *Oceanology,* **43,** 333–343.

——, ——, ——, and ——, 2003b: Modeling of internal soliton transformation on shelf of the Sea of Laptevykh. *Izv. Akad. Nauk. Arm. SSR, Ser. Tekh. Nauk.,* **4,** 3–16.

Rabinovich, M. I., and D. I. Trubetskov, 1989: *Oscillations and Waves in Linear and Nonlinear Systems*. Kluwer, 577 pp.

Stevens, C., and J. Imberger, 1994: Downward propagation internal waves generated at the base of the surface layer of a stratified fluid. *Geophys. Res. Lett.,* **21,** 361–364.

Sutherland, B. R., 2006: Weakly nonlinear internal gravity wavepackets. *J. Fluid Mech.,* **569,** 249–258.

Tabaei, A., T. R. Akylas, and K. Lamb, 2005: Nonlinear effects in reflecting and colliding internal wave beams. *J. Fluid Mech.,* **526,** 217–243.

Vlasenko, V., 1987: Generation of internal waves in stratified ocean of variable depth. *Izv., Acad. Sci., USSR, Atmos. Oceanic Phys. (Engl. Transl.),* **23,** 225–230.

——, N. Stashchuk, K. Hutter, and K. Sabinin, 2003: Nonlinear internal waves forced by tides near the critical latitude. *Deep-Sea Res. I,* **50,** 317–338.

——, ——, and ——, 2005: *Baroclinic Tides: Theoretical Modeling and Observational Evidence*. Cambridge University Press, 351 pp.